

Supplementary Data to Accompany:

**Energy-Resolved Collision-Induced Dissociation Pathways of
Model N-Linked Glycopeptides: Implications for Capturing Glycan Connectivity and
Peptide Sequence in a Single Experiment**

Venkata Kolli and Eric D. Dodds

Department of Chemistry, University of Nebraska – Lincoln

Lincoln, NE 68588-0304 USA

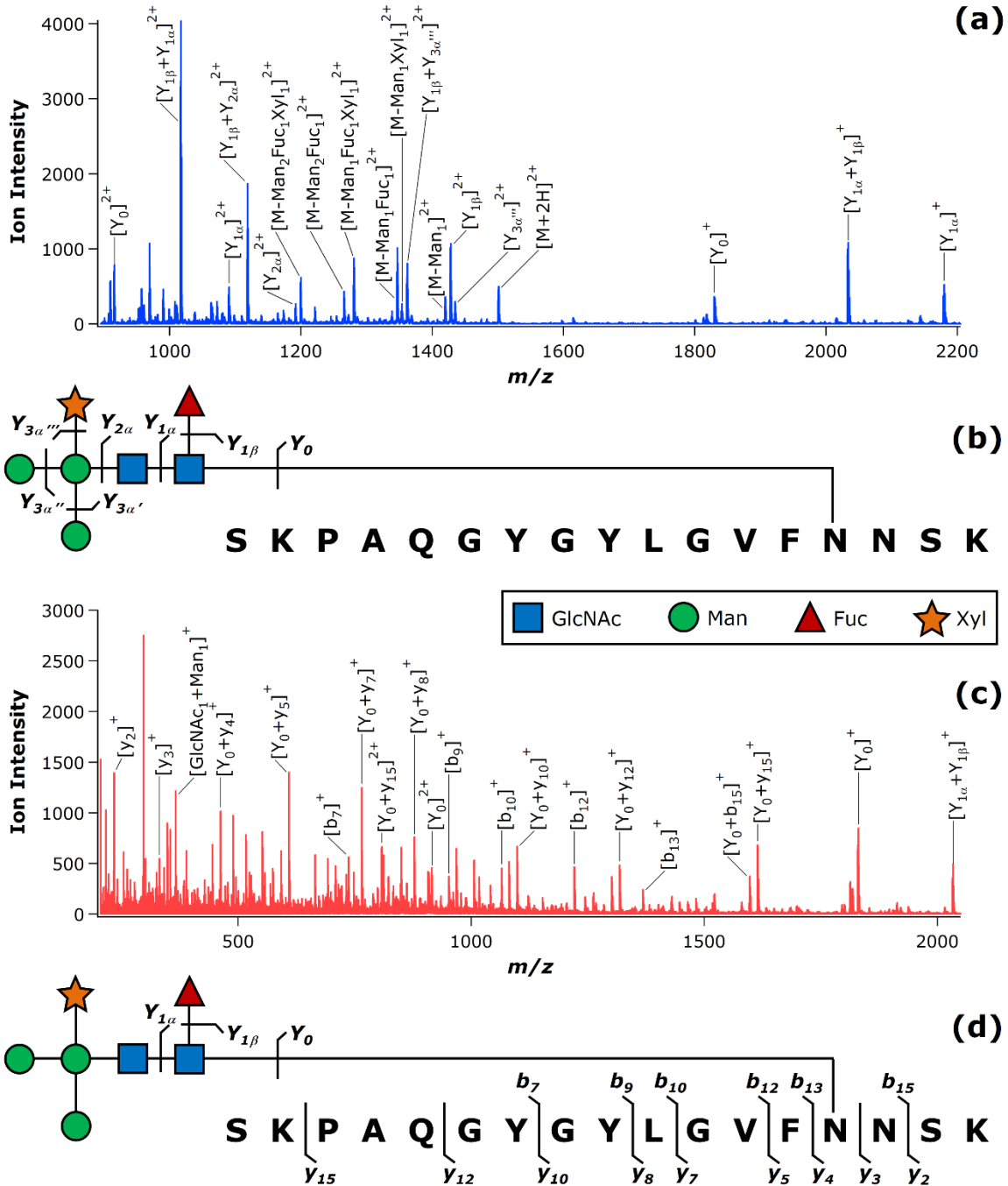


Figure S1. CID of the doubly protonated ECL glycopeptide. The CID spectrum acquired at $\Delta U = 47.5$ V **(a)** exhibited only glycan cleavage, as shown in the accompanying diagram **(b)**. The CID spectrum acquired at $\Delta U = 65.0$ V **(c)** exhibited mainly peptide fragments following glycan loss, as shown in the accompanying diagram **(d)**.

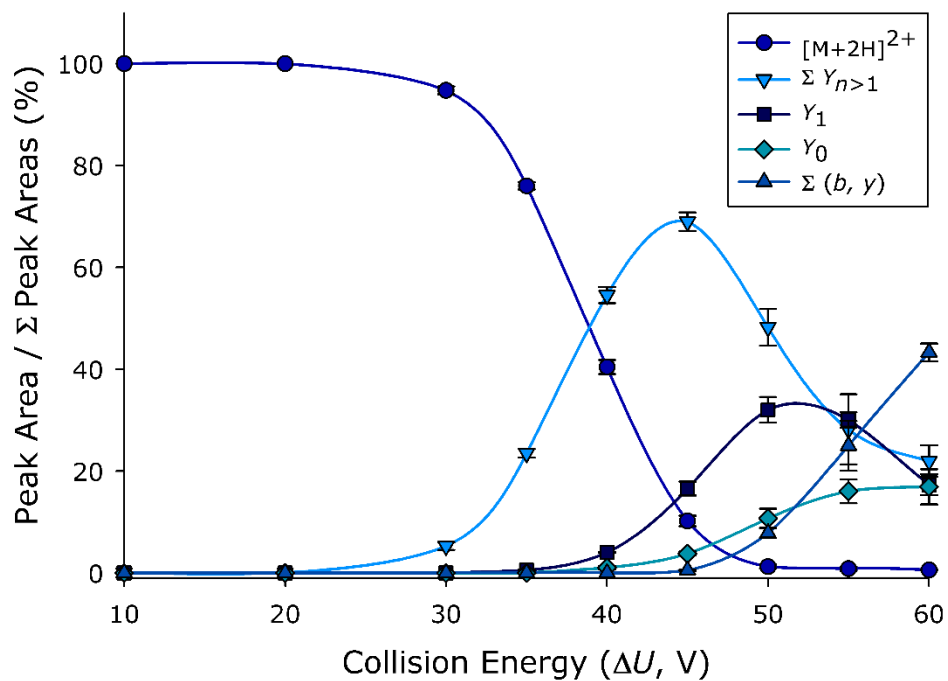


Figure S2. Energy-resolved CID plot for the doubly protonated ECL glycopeptide. The normalized peak area of each ion or group of ions is plotted as a function of the collision energy, expressed as the applied DC offset. Each data point represents the mean of three replicate measurements; error bars, where visible, represent the standard deviation.

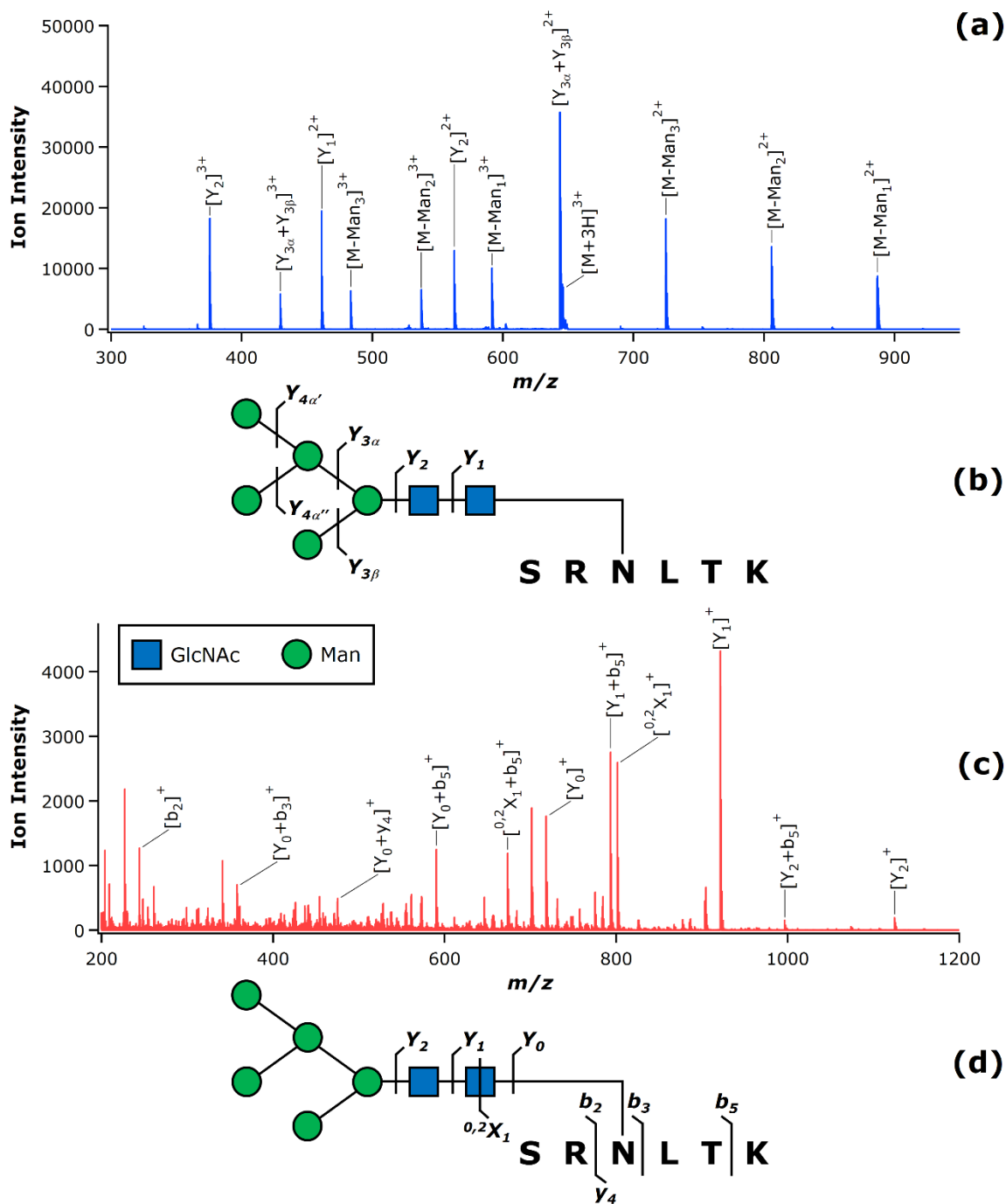


Figure S3. CID of the triply protonated BRB glycopeptide. The CID spectrum acquired at $\Delta U = 10.0$ V **(a)** exhibited only glycan cleavage, as shown in the accompanying diagram **(b)**. The CID spectrum acquired at $\Delta U = 40.0$ V **(c)** exhibited mainly peptide fragments following glycan loss, as shown in the accompanying diagram **(d)**.

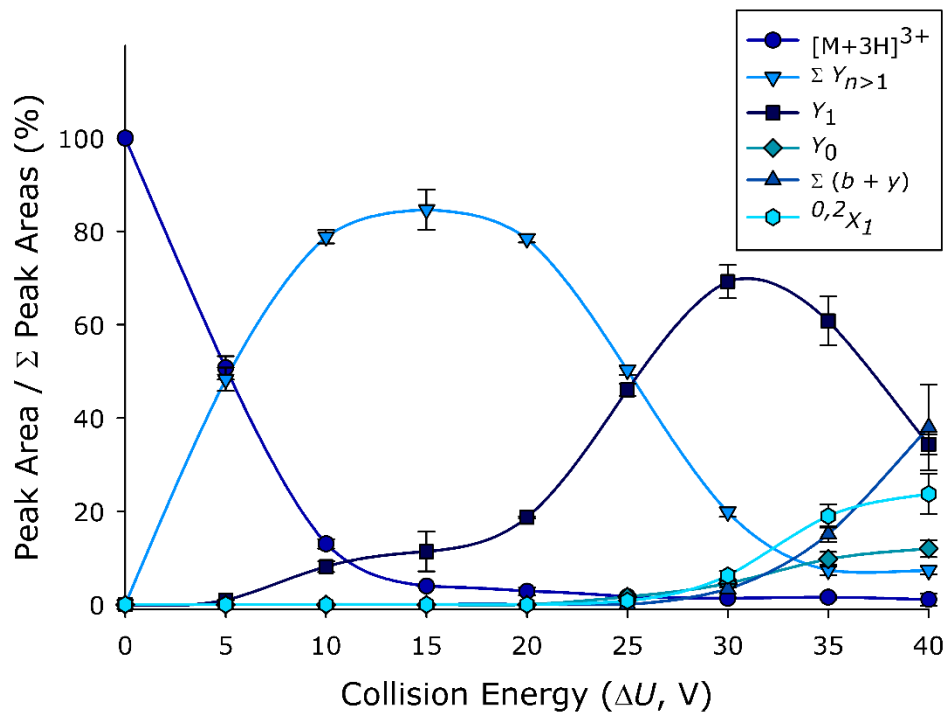


Figure S4. Energy-resolved CID plot for the triply protonated BRB glycopeptide. The normalized peak area of each ion or group of ions is plotted as a function of the collision energy, expressed as the applied DC offset. Each data point represents the mean of three replicate measurements; error bars, where visible, represent the standard deviation.

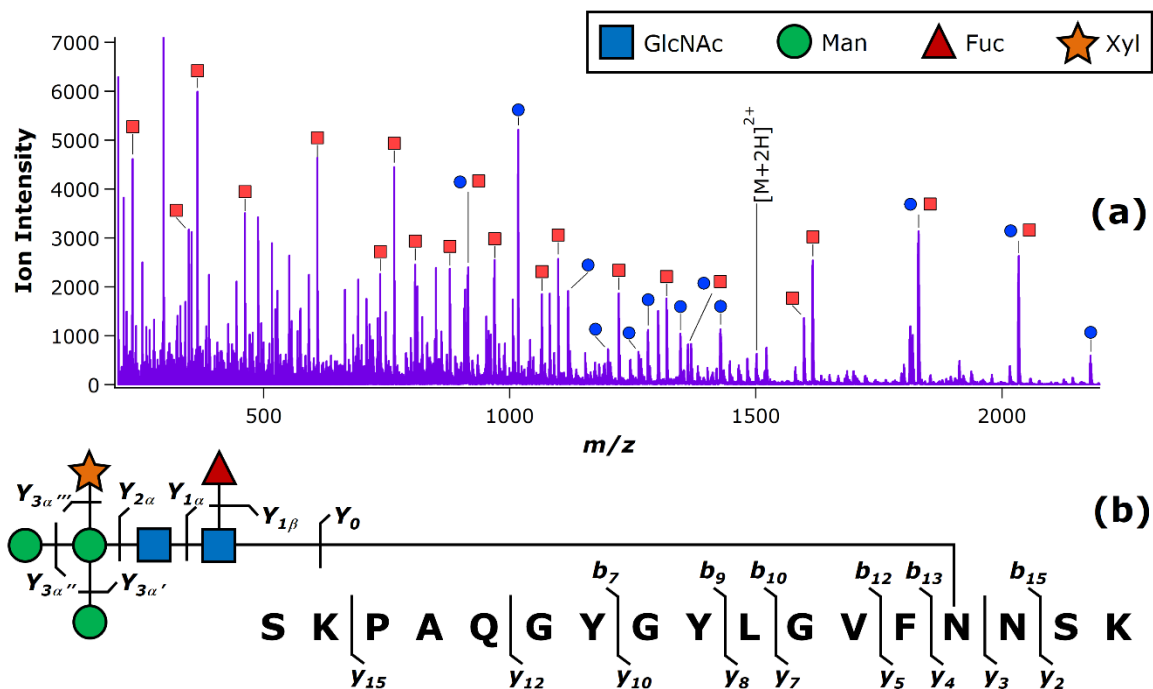


Figure S5. Multi-energy CID of the doubly protonated ECL glycopeptide. The CID spectrum **(a)** was acquired via online switching between two collision energies: $\Delta U = 47.5$ V and $\Delta U = 65.0$ V. These correspond to the collision energies applied in **Figure S1a** and **Figure S1c**, respectively. Peak assignments are the same as those shown in **Figure S1a** (labeled here with blue circles) and **Figure S1c** (labeled here with red squares). An abundance of both glycan and peptide fragments were observed, as shown in the accompanying diagram **(b)**.

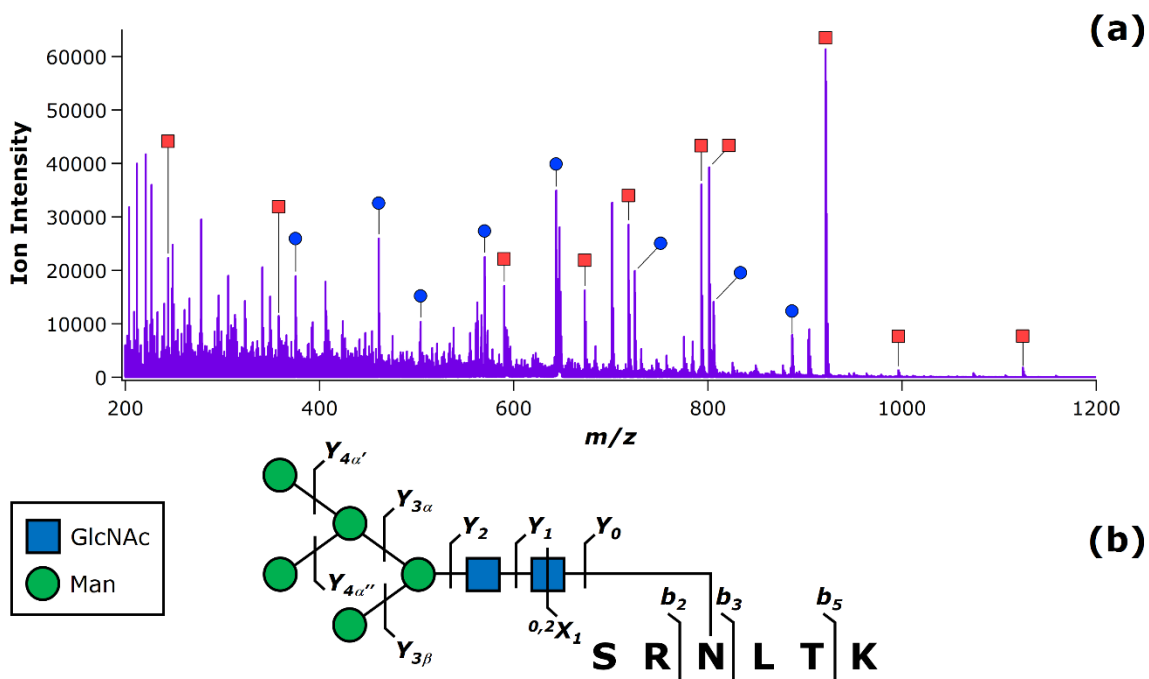


Figure S6. Multi-energy CID of the triply protonated BRB glycopeptide. The CID spectrum **(a)** was acquired via online switching between two collision energies: $\Delta U = 10.0$ V and $\Delta U = 40.0$ V. These correspond to the collision energies applied in **Figure S3a** and **Figure S3c**, respectively. Peak assignments are the same as those shown in **Figure S3a** (labeled here with blue circles) and **Figure S3c** (labeled here with red squares). An abundance of both glycan and peptide fragments were observed, as shown in the accompanying diagram **(b)**.

Table S1. CID collision energies (ΔU) corresponding to 50% precursor ion survival, and the corresponding precursor ion charge states (z) and vibrational degrees of freedom (f). The charge state and degrees of freedom corrected 50% precursor ion survival energies are given in the rightmost column, and have each been multiplied by a factor of 100 to yield more convenient figures. Within the glycopeptide compositions, amino acid residues with basic side chains are shown in bold, while the glycosylated asparagine residue is underlined. The number of charge-carrying protons (n_{H+}) are also indicated relative to the number of basic amino acid side chains (n_B).

	Glycopeptide Composition	z	f	ΔU (V)	$(z\Delta U/f)$ *100
$n_{H+} > n_B$	[SKPAQGYGYLGVF <u>N</u> SK +GlcNAc ₂ Man ₃ Xyl ₁ Fuc ₁ +3H] ³⁺	3	1230	14.9	3.63
	[SR <u>N</u> LTK +GlcNAc ₂ Man ₅ +3H] ³⁺	3	804	5.5	2.05
$n_{H+} = n_B$	[SKPAQGYGYLGVF <u>N</u> SK +GlcNAc ₂ Man ₃ Xyl ₁ Fuc ₁ +2H] ²⁺	2	1227	38.8	6.32
	[SR <u>N</u> LTK +GlcNAc ₂ Man ₅ +2H] ²⁺	2	801	26.2	6.54